N.M. Agababyan [1], V.V. Ammosov, M. Atayan [2], N. Grigoryan [2],
H. Gulkanyan [2], A.A. Ivanilov [*], Zh. Karamyan [2], V.A. Korotkov

THE CHARACTERISTICS OF NEUTRINONUCLEAR REACTIONS AT E_ν = 1–3 GeV

[1] Joint Institute for Nuclear Research, Dubna, Russia
[2] Yerevan Physics Institute, Armenia
[*] E-mail: ivanilov@ihep.ru

Abstract

Agababyan N.M., Ammosov V.V., Atayan M. et al. The Characteristics of Neutrinonuclear Reactions at $E_\nu = 1$–3 GeV: IHEP Preprint 2006–12. – Protvino, 2006. – p. 11, figs. 11, refs.: 7.

For the first time, the characteristics of the charged current neutrinonuclear interactions are investigated at $E_\nu = 1$–3 GeV using the data obtained with SKAT propane-freon bubble chamber irradiated in the neutrino beam at Serpukhov accelerator. The E_ν-dependence of the mean multiplicities of different types of secondary particles and their multiplicity, momentum and angular distributions are measured.

Аннотация

Агабабян Н.М., Аммосов В.В., Атаян М. и др.   Характеристики нейтрино-ядерных реакций при $E_\nu = 1$–3 ГэВ: Препринт ИФВЭ 2006–12. – Протвино, 2006. – 11 с., 11 рис., библиогр.: 7.

Впервые изучены характеристики нейтрино-ядерных реакций заряженного тока при $E_\nu = 1$–3 ГэВ на основе данных, полученных при экспозиции пузырьковой пропан-фреоновой камеры СКАТ в нейтринном пучке Серпуховского ускорителя. Измерена энергетическая зависимость средних множественностей различных типов вторичных частиц, а также их импульсные, угловые и множественные распределения.

1. Introduction

The experimental data on the characteristics of neutrinonuclear reactions at E_ν <3 GeV are of interest, in particular, in view of current and anticipated experiments on the neutrino oscillations (see, e.g., [1]). The detailed data are available only in the low energy range of E_ν <1 GeV, where the quasielastic reaction $\nu n \to \mu^- p$ on the nuclear neutrons dominates [2]. The aim of this work is to obtain, for the first time, detailed experimental data on neutrinonuclear reactions in the range of 1< E_ν <3 GeV. Section 2 is devoted to the experimental procedure of the selection of the neutrino interaction events and the reconstruction of the neutrino energy. The experimental results are presented in Section 3 and summarized in Section 4.

2. Experimental procedure

a) The event selection criteria

The experiment was performed with SKAT bubble chamber [3], exposed to a wideband neutrino beam obtained with a 70 GeV primary protons from the Serpukhov accelerator. The chamber was filled with a propan-freon mixture containing 87 vol% propane (C_3H_8) and 13 vol% freon (CF_3Br) with the percentage of nuclei H:C:F:Br = 67.9:26.8:4.0:1.3 %. The nuclear inter-action and radiation lengths of the mixture were $\lambda_I = 149$ cm and $X_0 = 50$ cm. The volume of the chamber was 6.5 m^3, the chosen fiducal volume 1.73 m^3. A 20 kG uniform magnetic field was provided within the operating chamber volume.

Charged current interactions, containing a negative muon were selected. A muon was iden-tified as a particle that possessed the highest transverse momentum among negative particles and did not suffer a secondary interaction in the chamber. Other negatively charged particles were considered to be π^- mesons. The overwhelming part of protons with momentum below 0.6 GeV/c and a fraction of those with momentum up to 0.85 GeV/c were identified by their stopping in the chamber. Other positively charged particles were assumed to be π^+ mesons, except for cases explained below.

In order to reduce the uncertainty in reconstructing the neutrino energy E_ν, the events were selected for which errors in measuring the momenta of all charged secondaries and converted photons were less than 27% and 100%, respectively. The mean relative error $< \Delta p/p >$ in the momentum measurement for muons, protons, pions and gammas was, respectively, 4%, 6%, 10%

1

and 21%. Each selected event was assigned a weight that took into account loss of events. The mean weight of the sample used in the present study was 1.18.

To diminish the background induced by neutral and charged particles, the following requirements were imposed on selected events:

- The net charge of secondary hadrons is positive.

- The visual energy of neutrino $E_\nu^{vis} = E_\mu + \nu_{vis} > 0.6$ GeV, where E_μ is the muon energy, ν_{vis} is the visual energy transferred to hadrons (including decay photons and neutral strange particles, if any).

- The value of the summary momentum $\overrightarrow{p}$ of detected secondary particles was $| \overrightarrow{p} | > 0.7$ GeV/c, while its longitudinal component p_L (with respect to the neutrino direction) exceeded the transverse component p_T (the latter coinciding with the summary transverse momentum of undetected secondary particles).

- The minimal neutrino energy defined from the kinematics of the quasielastic reaction $\nu n \to \mu^- p$, $E_\nu^{el} = (m_N E_\mu - 0.5 m_\mu^2)/(m_N - E_\mu + p_\mu \cos \vartheta_\mu)$, did not exceed more than by 30% [2] the upper limit (3 GeV) of the considered range of E_ν: $E_\nu^{el} < 3.9$ GeV. Here m_N and m_μ are the proton and muon masses, p_μ and ϑ_μ are the muon momentum and angle with respect to the neutrino.
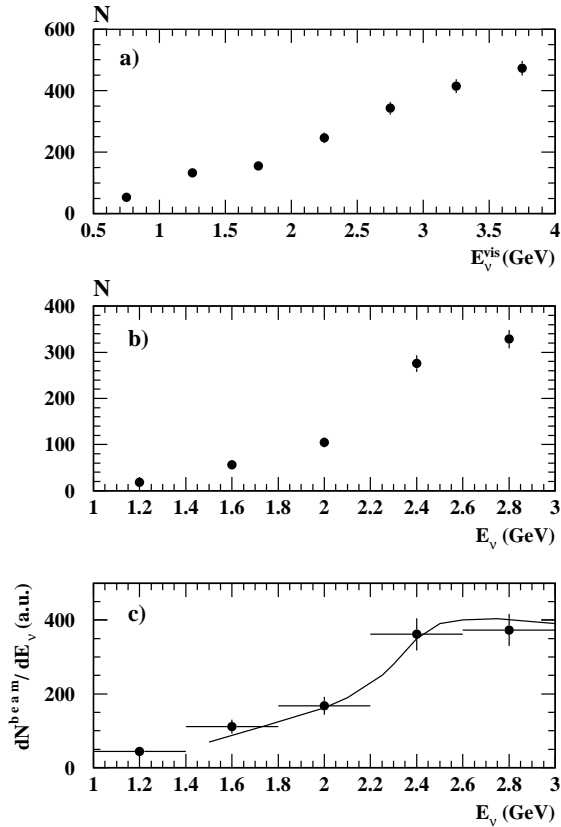

Figure 1. The distribution on: E_ν^{vis} for selected events (a), the reconstructed neutrino energy (b), the reconstructed energy of the beam neutrino (c). The curve is taken from [6].

2

The distribution on E_ν^{vis} for selected events in the range $0.7 < E_\nu^{vis} < 4$ GeV is shown in Fig. 1a. The measured value of E_ν^{vis} is, in general, the minimal value of the true neutrino energy, and hence to be corrected for the contribution from undetected gammas and neutrons. An exception are the events satisfying the kinematics of exclusive reactions without secondary neutral particles (see the next subsection). For a part of these events, E_ν can be even smaller than E_ν^{vis} provided that the proton hypothesis for an unidentified positive particle matches better the kinematics of an exclusive channel, than the π^+ hypothesis.

b) The identification of exclusive channel

In order to avoid a unnecessary energy correction for undetected secondaries, each event was analysed for its belonging to the following exclusive channels without neutral secondaries:

$$
\begin{align}
\nu n &\rightarrow \mu^- p \tag{1}\\
\nu p &\rightarrow \mu^- p\, \pi^+ \tag{2}\\
\nu n &\rightarrow \mu^- p\, \pi^+\pi^- \tag{3}
\end{align}
$$

with an arbitrary number of accompanying identified protons (originating from the nuclear cascading). In (1)-(3), p (π^+) stands for an identified proton (π^+ meson) or a positively charged particle to be identified as a proton or π^+ meson from the kinematical fit.

Figs. 2a and 2b show the distributions on the azimutal angle ϕ between vectors $\overrightarrow{p}_\mu$ and $\overrightarrow{p}_h = \overrightarrow{p} - \overrightarrow{p}_\mu$ in the transverse plane and on the squared transverse momentum p_T^2 for events topologically consistent with reactions (1)-(3). The observed peaks near $\phi \sim 180°$ and $p_T^2 \sim 0$ indicate on a significant fraction of events satisfying the kinematics of reactions (1)-(3). For further analysis the events with $\phi > 155°$ and $p_T^2 < 0.15$ (GeV/c)^2 were selected, the chosen boundaries roughly corresponding to violation of the kinematics of reactions (1)-(3) due to the Fermi-motion of the target nucleon and the measurement errors. For these events, the distribution on the dimensionless variable $r_L = (E_\nu^{vis} - p_L)/E_\nu^{vis}$, characterizing the longitudinal momentum-energy disbalance of the reaction, is plotted in Fig. 2c. As it is seen, the distribution is strongly peaked at $r_L \approx 0$. The events with $|r_L| < 0.15$ were assumed to be belonging to the exclusive reactions (1)-(3). The number of these events is 126 (the weighted number 140.2), the distribution of which on E_ν is plotted in Fig. 2d and, separately for channels (1), (2) and (3), in Fig. 2e. The curves in this figure are obtained by approximation of available experimental data for νp and νn interactions [4] (taking into account the proton and neutron contents of the target nuclei) convoluted with the expected neutrino flux spectrum on the bubble chamber SKAT [5]. The normalization of these curves is chosen to fit our data on the main exclusive channel (1). As a result, the predictions for channels (2) and (3) overestimate the data, probably due to the intranuclear interaction effects for pions produced in the primary νN interaction (see Section 3 below).

The distribution on the invariant mass W of the hadronic system for exclusive channels (1) and (2) is shown in Fig. 2f. The clear peak at $W \approx m_N$, with a typical width ~ 0.15 GeV (caused by Fermi-motion and measurement errors), corresponds to the quasielastic reaction (1). The W-distribution for the reaction (2) reflects probably the production of the Δ^{++} states.
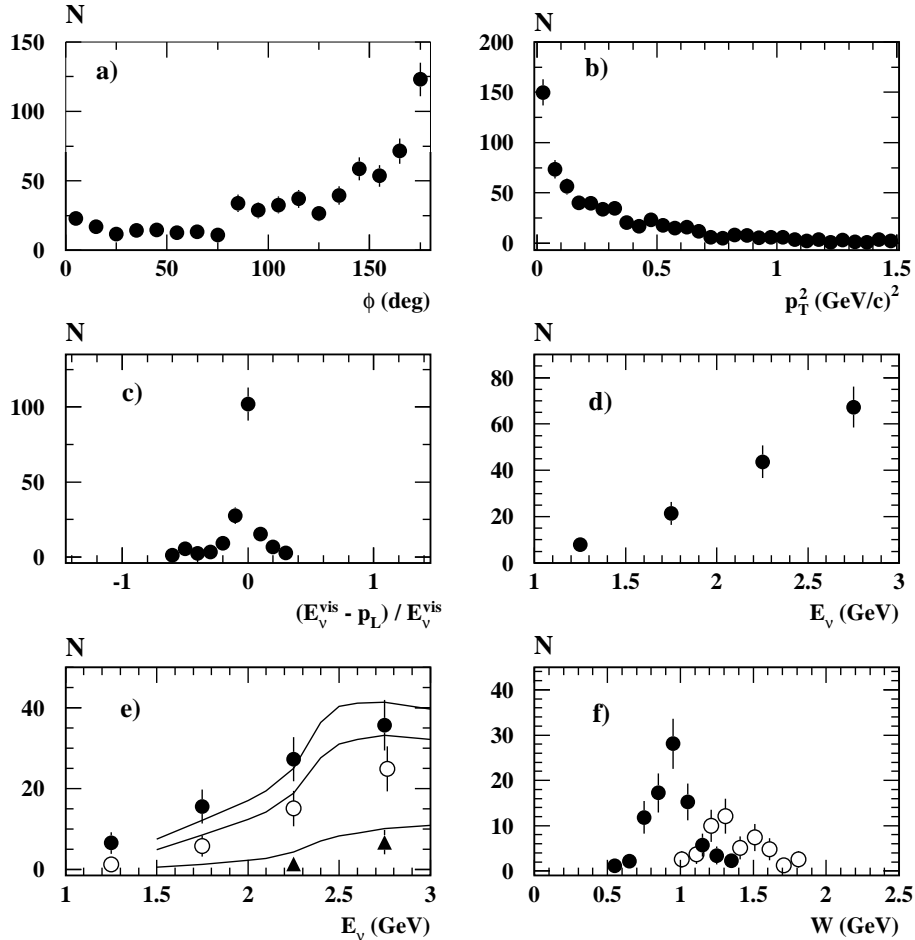
3

Figure 2. The distribution for events-candidates for exclusive channels on: the azimutal angle ϕ between the momenta of the muon and the hadronic system (a); squared transverse momentum p_T^2 (b); ratio $(E_\nu^{vis} - p_L)/E_\nu^{vis}$ for events with $\phi > 155°$ and $p_T^2 < 0.15$ $(GeV/c)^2$ (c); E_ν for exclusive channels (1)-(3) (d); E_ν for channels: (1) (full circles), (2) (empty circles) and (3) (triangles) (e); invariant hadronic mass W for exclusive channels (1)-(3) (full circles) and the channel (2) (empty circles) (f).

c) The reconstruction of the neutrino spectrum

Only a small part (about 28%) of the total event sample can be identified as exclusive channels (1)-(3). The rest part contains undetected secondaries, for which a correction has to be introduced to estimate E_ν. The mean value ν of the corrected energy transferred to hadrons (at given narrow intervals of ν_{vis}) is approximated as $\nu = a + b\nu_{vis}$, where the coefficients a and b are found by means of the procedure applied in [6]: $a = 0.15 \pm 0.24$ GeV, $b = 1.07 \pm 0.05$ at $E_\nu^{vis} > 2$ GeV and $a = 0.5 \pm 0.3$ GeV, $b = 1.5 \pm 0.4$ at $E_\nu^{vis} < 2$ GeV. The reconstructed spectrum of E_ν in the range 1 - 3 GeV is presented in Fig. 1b, while Fig. 1c shows the spectrum of the beam neutrino evaluated using the total cross sections [7] of reactions $\nu p \to \mu^- X$ and $\nu n \to \mu^- X$ and taking into account the proton and neutron content of the target nuclei. As it is seen, the latter spectrum is consistent with the expected neutrino flux spectrum (at $E_\nu > 1.5$ GeV) on the bubble chamber SKAT [5].

4

3. Experimental results

a) The E_ν-dependence of the mean characteristics of produced particles

Fig. 3 presents the E_ν-dependence of mean multiplicities of secondary particles: protons, π^+ mesons, π^- mesons, charged pions, γ-quanta, π^0 mesons and neutral strange particles (V^0). The mean value of $< n_{\pi^0} >$ is estimated as $< n_{\pi^0} >= 0.5 < n_\gamma > \bar{w}_\gamma$, where $\bar{w}_\gamma$ is the mean weight of detected γ's defined by their conversion probability in the chamber. As it is seen, all multiplicities increase with E_ν, except the mean multiplicity of identified protons, probably due to the fact that, with increasing E_ν, a larger fraction of recoil protons acquires momenta $p_p > 0.6$ GeV/c and hence can be detected as a unidentified positive particle. The contribution of these protons is partly taken into account in Fig. 3a, where the full circles stand for $< n_p >$ including also 'kinematically' identified protons from reactions (1)-(3). The latter will be included below in the all data concerning protons. The solid curves in Figs. 3b, 3c and 3f are the approximation of the experimental data [4] on the mean multiplicities of π^+, π^- and π^0 mesons in νN interactions. It is seen, that the values of $< n_{\pi^+} >$ at $E_\nu = 2.3$ - 3 GeV exceed those in νN interactions, probably due to a significant ($\sim 30\%$) contamination from the unidentified protons. On the other hand, the values of $< n_{\pi^+} >$ at $E_\nu = 1$ - 1.9 GeV and $< n_{\pi^-} >$ and $< n_{\pi^0} >$ in the whole E_ν range are reduced as compared to those in νN interactions. This reduction can be, at least partly, attributed to the absorption of pions on a pair of nucleons within the nucleus, $\pi(NN) \to (NN')$. The dashed curves in Figs. 3b, 3c and 3f are the results of calculations incorporating this process (see for details [2] and references therein). As it is seen, the predictions are in reasonably agreement with the data on $< n_{\pi^+} >$ at $E_\nu = 1$ - 1.9 GeV, as wel as on $< n_{\pi^-} >$ and $< n_{\pi^0} >$ in the whole energy interval, especially if one takes into account the uncertainties (reaching $\pm 20\%$) in the approximation of the experimental data on the mean multiplicity of pions in νN interactions.

The E_ν-dependence of the mean momentum of different types of particles is presented in Fig. 4. This dependence is more expressed for charged pions and especially for muons, being rather moderate for protons and gammas. Fig. 5 shows the E_ν - dependence of the mean fraction f_i of the neutrino energy transferred to the muon ($f_\mu = E_\mu/E_\nu$), protons ($f_p = \sum T_p/E_\nu$), charged pions ($f_\pi = \sum E_\pi/E_\nu$), detected gammas ($f_\gamma = \sum E_\gamma/E_\nu$) and undetected neutral particles ($f_{miss} = (\nu - \nu_{vis})/E_\nu$). It is seen, that f_μ depends on E_ν rather weekly, being enclosed between $0.41 < f_\mu < 0.47$. The proton contribution smoothly decreases from $f_p = 0.13$ to 0.05, while that for charged pions increases from $f_\pi = 0.12$ to 0.32. The contribution of the detected gammas is very small, amounting $f_\gamma = 0.01$ - 0.04, and increases with E_ν. The energy fraction carried by the undetected neutral particles is determined with a large uncertainty (due to the large errors in parameters a and b, cf. Section 2) and tends to decrease from $f_{miss} \sim 0.3$ up to ~ 0.1 with increasing E_ν.

The mean values of the invariant mass W of the hadronic system and the squared transfer momentum Q^2 are plotted in Fig. 6. A significant rise of $< Q^2 >$ is observed, while the E_ν-dependence of $< W >$ is rather weak.
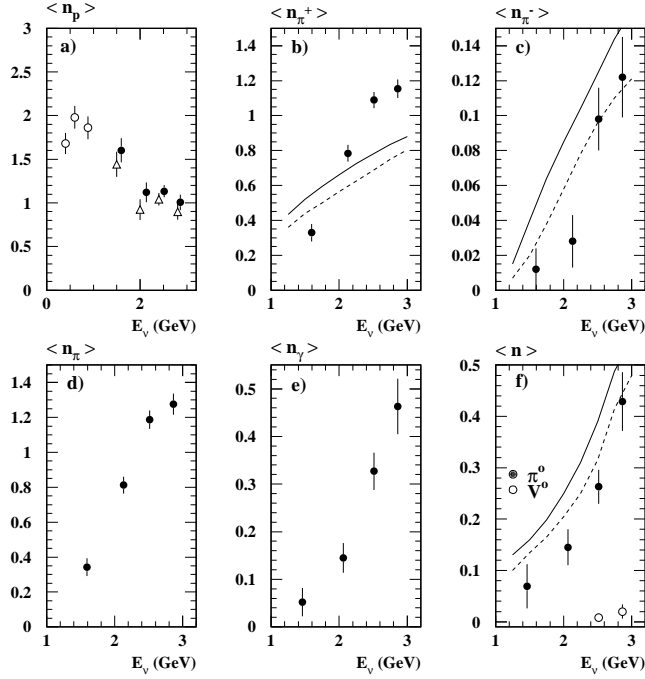
Figure 3. The E_ν-dependence of the mean multiplicity of: identified protons (empty circles [2] and triangles) and protons, including 'kinematically' identified ones (full circles) (a); π^+ mesons (b); π^- mesons (c); charged pions (d); γ- quanta (e); π^0 mesons (full circles) and V^0 (empty circles) (f). The solid curves are the approximation of the experimental data on the mean multiplicities of pions in νN interactions, while the dashed curves are those when taking into account the intranuclear absorption of pions (see the text).
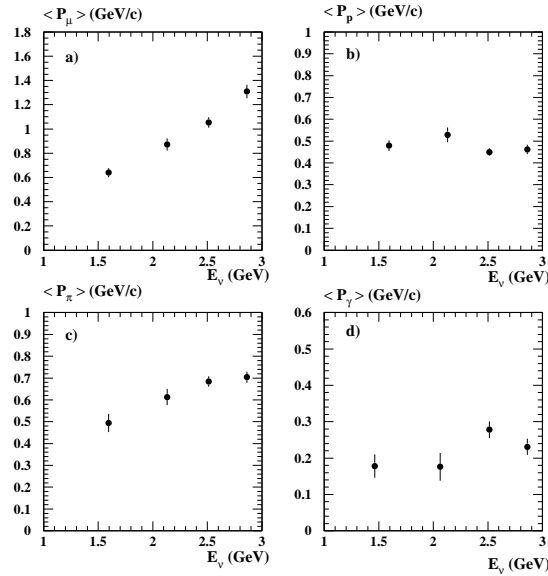
Figure 4. The E_ν-dependence of the mean momentum of: muons (a); protons, including 'kinematically' identified ones (b); charged particles, excluding identified protons (c); γ-quanta (d).

6
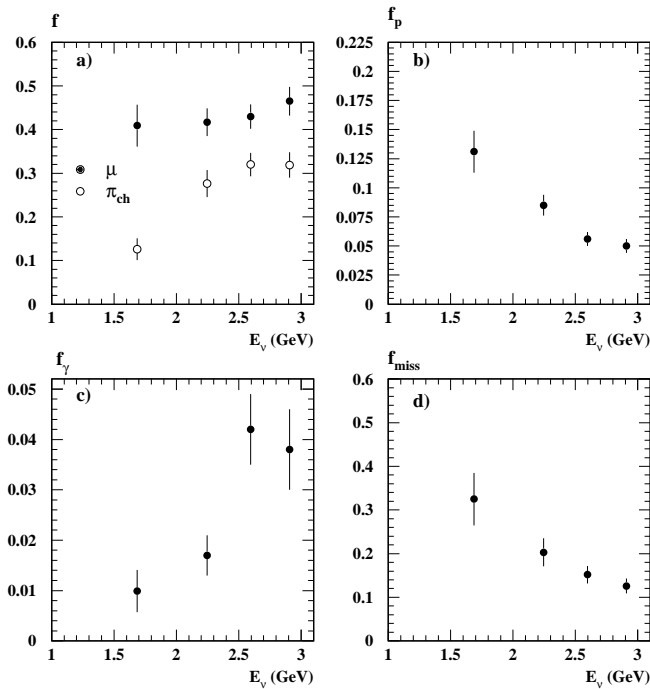
Figure 5.   The E_ν-dependence of the mean energy fracton of the neutrino carried by: muons and charged pions (a); protons (b); γ-quanta (c); undetected neutral particles (d).
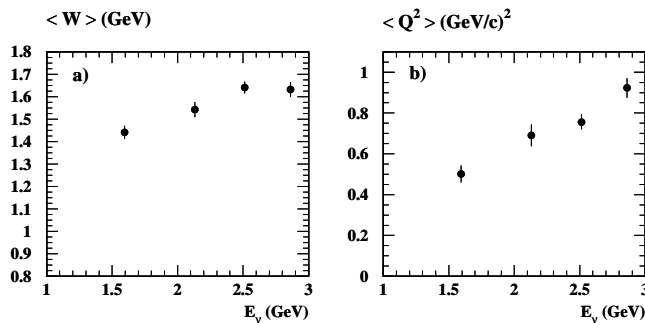
Figure 6.   The E_ν-dependence of the mean values of W (a) and Q^2 (b).

b) The multiplicity, momentum and angular distributions of produced particles

Figs. 7a - 7f present the multiplicity and momentum distributions for protons, as well as separately for those produced in the forward ($cos\theta_p > 0$) and backward ($cos\theta_p <0$) directions with respect to the neutrino beam. These distributions, as well as the proton angular distribution (Fig. 7g), are presented for the whole range of $E_\nu = 1$ - 3 GeV, because the characteristics of protons were found to not depend noticeably on E_ν. The multiplicity distributions, shown in Figs. 7a - 7c, are compared with the poissonian distributions calculated at the measured values of $< n_p > = 1.17 \pm 0.05$, $< n_p > = 0.83 \pm 0.04$ (at $cos\theta_p > 0$) and $< n_p > = 0.33 \pm 0.02$ (at $cos\theta_p < 0$). As it is seen, the tail of experimental distridutions deviates from the poissonian one. The momentum distributions (Figs. 7d - 7f) can be roughly approximated by the dependence $\sim exp(-\alpha p^2)$ with $\alpha = 3.5 \pm 0.2$ (at all $cos\theta_p$), 2.8 ± 0.2 (at $cos\theta_p > 0$) and 4.6 ± 0.4 $(GeV/c)^{-2}$ (at $cos\theta_p < 0$). The distribution on $cos\theta_p$ (Fig. 7g) exhibits a linear dependence $\sim 1 + \beta cos\theta_p$ with a slope parameter $\beta = 0.82 \pm 0.05$.
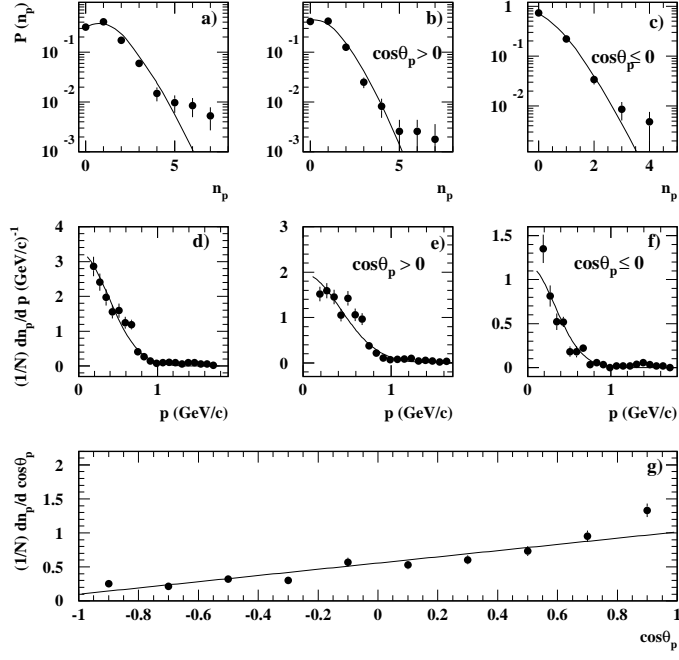
7

Figure 7.   The multiplicity and momentum distributions for protons (a and d); protons with $cos\theta_p > 0$ (b and e) and $cos\theta_p < 0$ (c and f); the distribution on $cos\theta_p$ (g).
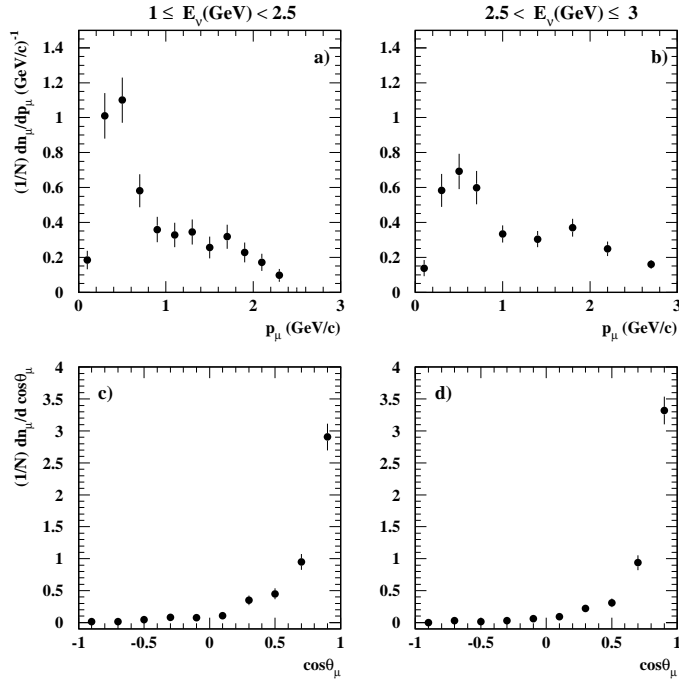

Figure 8.   The momentum and angular distributions of muons for two E_ν intervals.

8

Figs. 8 and 9 show the momentum and angular distributions of muons and charged pions in two intervals of $E_\nu = 1 - 2.5$ and $2.5 - 3$ GeV with approximately equal statistics. The momentum distribution of muons (Figs. 8a and 8b) is peaked at $p_\mu \sim 0.5$ GeV/c and falls steeply with increasing p_μ for the range $E_\nu = 1 - 2.5$ GeV, being, however, much flatter for the range $E_\nu = 2.5 - 3$ GeV. The angular distribution of muons is similar for both E_ν ranges, being strongly peaked at $cos\theta_\mu \sim 1$. The momentum distribution of pions is also peaked at $p_\pi \sim 0.5$ GeV/c and falls (more steeply for the range $E_\nu = 1 - 2.5$ GeV) with increasing p_π. Their angular distribution is peaked at $cos\theta_\mu \sim 1$ (more strongly for the range $E_\nu = 2.5 - 3$ GeV).
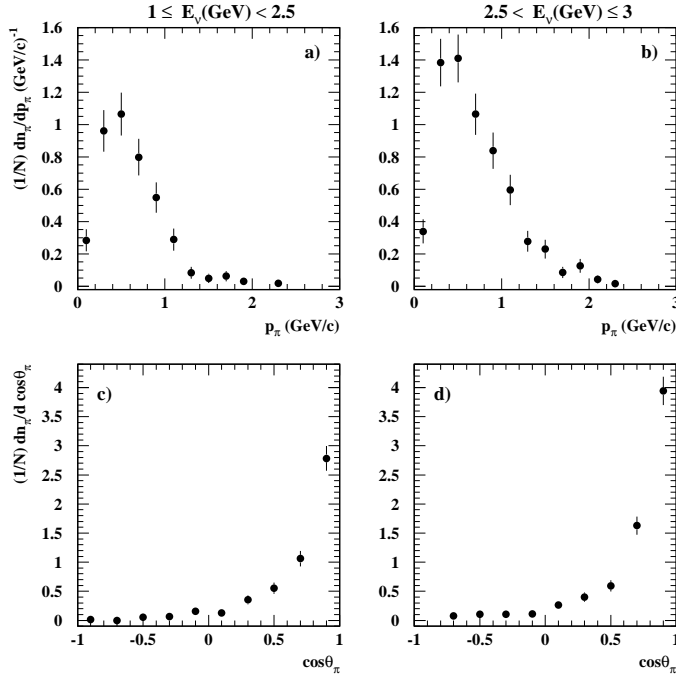

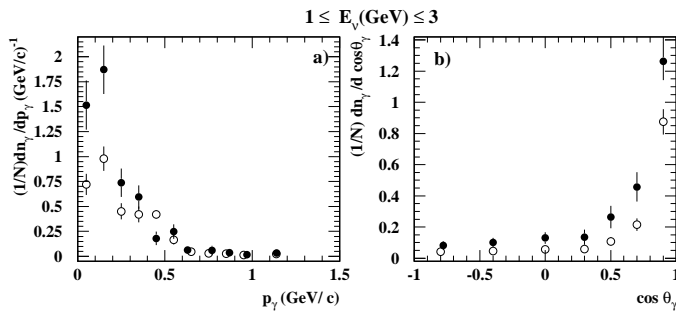Figure 9. The momentum and angular distributions of charged pions for two E_ν intervals.

Figure 10. The momentum and angular distributions of γ- quanta corrected (close circles) and not corrected (open circles) for their detection efficiency.

9

The momentum and angular distributions of γ- quanta, both corrected and not corrected for their detection efficiency, are shown in Fig. 10, but now, due to the lack of their statistics, for the whole range of E_ν = 1 - 3 GeV. The momentum distribution has a maximum at $p_\gamma \sim 0.15$ GeV/c (more than twice smaller than that for charged pions), while the angular distribution is somewhat shifted toward larger angles as compared to that for charged pions.

Finally, the distributions on W and Q^2 are plotted in Fig. 11 for two E_ν intervals. Due to a limited resolution of W, as well as the effects of the secondary intranuclear interactions, its distribution extends to the region below the nucleon mass. Besides, no peak is seen at $W \approx m_N$, due to a small contribution of the identified events of the quasielastic reaction (1) as compared to the non-identified one.
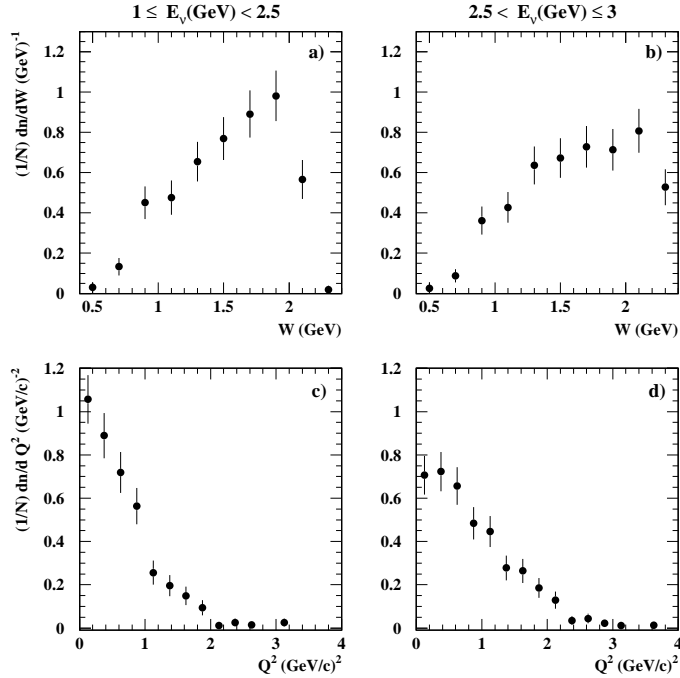

Figure 11.   The distributions on W (a) and Q^2 (b).

4. Summary

The charged current neutrinonuclear reactions at E_ν = 1 - 3 are investigated using the data obtained with SKAT propane-freon bubble chamber irradiated in the neutrino beam at Serpukhov accelerator. The reconstructed neutrino spectrum is found to be consistent with the expected one on the bubble chamber.

For the first time, in this E_ν range detailed experimental data are obtained on the characteristics of the produced particles. The E_ν - dependence of the mean multiplicities of protons, charged pions, γ- quanta, π^0 mesons and neutral strange particles and their multiplicity, momentum and angular distributuions are measured. An indication is obtained, that the yield of pions in the neutrinonuclear interactions is reduced as compared to that in νN interactions, which can be qualitatively explained by their absorption in the nuclear medium.

10

References

[1] Y.Oyama, KEK Preprint 2001-7 (2001); T.Ishii, KEK Preprint 2002-28 (2002); S.H.Ahn et al., Phys. Lett. **B 511**, 178 (2001).

[2] N.M.Agababyan et al., YerPhI Preprint-1581(2) (2003).

[3] V.V.Ammosov et al., Fiz. Elem. Chastits At. Yadra **23**, 648 (1992) [Sov. J. Part. Nucl. **23**, 283 (1992)].

[4] S.I.Aleshin et al., Compilation of cross sections IV, CERN-HERA 87-01 (1987).

[5] D.S.Baranov et al., Phys. Lett.**81 B**, 255 (1979).

[6] A.E.Asratyan et al., Yad. Fiz. **41**, 1193 (1985) [Phys. At. Nucl. **41**, 763 (1985)].

[7] N.J.Baker at al., Phys. Rev. **D 25**, 617 (1982).